CMS Physics Analysis Summary

Contact: cms-pag-conveners-susy@cern.ch 2012/11/18

Search for supersymmetry in events with same-sign dileptons and b-tagged jets with 8 TeV data

The CMS Collaboration

Abstract

A search for new physics is performed using events with isolated same-sign leptons and at least two b-quark jets in the final state. Results are based on a sample of proton-proton collisions at a center-of-mass energy of 8 TeV collected with the CMS detector and corresponding to an integrated luminosity of 10.5 fb^{-1}. No excess above the standard model background is observed. Upper limits are set on the number of events from non-standard-model sources and are used to constrain a number of new physics models. Information on acceptance and efficiencies is also provided so that the results can be used to confront additional models in an approximate way.

1 Introduction

Events with same-sign, isolated leptons (e or μ) from standard model (SM) processes in proton-proton collisions are extremely rare. As a result, searches for anomalous production of same-sign dileptons can be very sensitive to new physics contributions. These include supersymmetry (SUSY) [1–3], universal extra dimensions [4], pair production of $T_{5/3}$ (a fermionic partner of the top quark) [5], heavy Majorana neutrinos [6], and same-sign top-pair production [7, 8]. More specifically, the signature of same-sign dileptons accompanied by bottom quarks can arise from SUSY processes where third-generation quark superpartners are lighter than other squarks [9–13], resulting in an abundance of top and bottom quarks produced in cascade decays. These scenarios are particularly interesting for two reasons. First, because they have not been excluded by early SUSY searches at the Large Hadron Collider (LHC); second, because relatively light bottom and top squarks are necessary if SUSY is to be the "natural", i.e., not fine-tuned, solution to the gauge hierarchy problem (see for example the discussion in Ref. [12]).

In this PAS we present the result of a search for new physics in events with same-sign isolated dileptons and two or more b jets. The search was performed on a dataset corresponding to an integrated luminosity of 10.5 fb^{-1} of proton-proton (pp) collisions at a center-of-mass energy of 8 TeV collected with the Compact Muon Solenoid (CMS) [14] detector. This search is an extension of the search at a 7 TeV center-of-mass energy described in Ref. [15].

In the analysis we select events with two isolated, high transverse momentum (p_{T}), same-sign leptons and at least two b-tagged jets. The event counts in a number of signal regions, defined in terms of additional requirements on missing transverse energy ($E_{\mathrm{T}}^{\mathrm{miss}}$), the number of b-tagged jets, and the scalar sum of jet p_{T} (H_{T}), are compared with expectations from the standard model. Having found no evidence for a beyond-the-SM contribution to the event count, we set limits on the number of events from new physics in the event sample. These limits are then translated into a limit on the same-sign top-pair cross section and are used to bound the parameters of other new physics models. Finally, we include enough information on the event selection efficiencies to allow our results to be reinterpreted in other models of new physics.

2 The CMS detector

The central feature of the CMS apparatus is a superconducting solenoid, of 6 m internal diameter, providing a field of 3.8 T. The CMS experiment uses a right-handed coordinate system, with the origin defined to be the nominal interaction point, the x axis pointing to the center of the LHC ring, the y axis pointing up (perpendicular to the LHC plane), and the z axis pointing in the counterclockwise beam direction. The polar angle θ is measured from the positive z axis and the azimuthal angle ϕ is measured in the x-y (transverse) plane. The pseudorapidity η is defined as $\eta = -\ln[\tan(\theta/2)]$. Within the field volume are a silicon pixel and strip tracker, a crystal electromagnetic calorimeter, and a brass-scintillator hadron calorimeter. Muons are measured in gas-ionization detectors embedded in the steel return yoke. Full coverage is provided by the tracker, calorimeters, and the muon detectors within $|\eta| < 2.4$. Additional coverage is provided by endcap detectors out to $|\eta| = 3$, and by extensive forward calorimetry out to around $|\eta| = 5$. A more detailed description can be found in Ref. [14].

3 Event selection and Monte Carlo simulation

The event selection is essentially the same as for the 7 TeV analysis of Ref. [15]. We require two isolated same-sign leptons (e or μ) with pair invariant mass above 8 GeV, and at least two b-tagged jets. The kinematic requirements on jets and leptons are summarized in Table 1. Events with a third lepton of $p_{\mathrm{T}} > 10$ GeV that passes looser requirements and forms an opposite-sign same-flavor pair of invariant mass between 76 and 106 GeV with any of the two leptons are rejected. This last requirement is designed to minimize multi-boson backgrounds (WZ and ZZ events). Background from processes involving a $\gamma^\star$ or low-mass bound state is suppressed by rejecting events with a third loose lepton of $p_{\mathrm{T}} > 5$ GeV that forms an opposite-sign same-flavor pair of invariant mass less than 12 GeV.

Table 1: Kinematic requirements for jets and leptons in this analysis.

	p_{T}	η
electrons	$p_{\mathrm{T}} > 20$ GeV	$\lvert\eta\rvert < 1.442$ or $1.566 < \lvert\eta\rvert < 2.4$
muons	$p_{\mathrm{T}} > 20$ GeV	$\lvert\eta\rvert < 2.4$
jets	$p_{\mathrm{T}} > 40$ GeV	$\lvert\eta\rvert < 2.4$
b-tagged jets	$p_{\mathrm{T}} > 40$ GeV	$\lvert\eta\rvert < 2.4$

With respect to Ref. [15], there have been small modifications in the lepton identification and isolation requirements; the main difference is that lepton isolation is now computed using particle-flow information [16] rather than charged tracks and calorimeter deposits, and, more importantly, an event-by-event correction has been applied to account for the effect of multiple pp interactions in the same bunch crossing. This correction is based on a measurement of the hadronic event activity not associated with the pp interaction that produced the leptons (the mean number of interactions in the same beam crossing is 15).

The jet reconstruction is the same as in Ref. [15], but the b-tagging algorithm has been changed slightly. We now use the CSV method of Ref. [17], which is based on the combination of secondary vertex reconstruction and track-based lifetime information. Efficiencies for lepton identification, trigger efficiency, and b tagging are summarized in Section 7.

Monte Carlo simulations are used to estimate some of the SM backgrounds (see Section 4), as well as to calculate the efficiency for various new physics scenarios. In this analysis SM background samples and new physics signal samples are generated with the MADGRAPH [18] and PYTHIA [19] programs, respectively. Standard Model processes are simulated using a GEANT4-based model [20] of the CMS detector; the simulation of new physics signals is performed using the CMS fast simulation package [21]. Simulated events are then processed with the same chain of reconstruction programs used for collision data.

4 Backgrounds

There are three sources of SM backgrounds to the event selection:

- "fake leptons", i.e., leptons from heavy-flavor decay, misidentified hadrons, muons from meson decay in flight, or electrons from unidentified photon conversions. These are estimated from a sample of events with at least one lepton that passes a loose selection but fails the full set of tight identification and isolation requirements. The background estimation uses the "tight-to-loose" ratio, i.e., the probability for a loosely identified fake lepton to also pass the full set of requirements, as determined from studies of fake leptons in jet events.

- "charge flips", i.e., events with opposite-sign isolated leptons where one of the leptons is an electron and its charge is misreconstructed due to severe bremsstrahlung in the tracker material (this effect for muons is negligible). Charge flips are estimated by selecting opposite-sign ee or eμ events passing the full kinematic selection, weighted by the p_{T} and η dependent probability of electron-charge misassignment. This probability is obtained from Monte Carlo simulation and is validated on a sample of $\mathrm{Z} \to \mathrm{ee}$ events.
- rare SM processes that yield same-sign high-p_{T} leptons and b jets, mostly from $\mathrm{t\bar{t}W}$ and $\mathrm{t\bar{t}Z}$ production. This background contribution is obtained from Monte Carlo simulation.

More details on the background estimation can be found in Refs. [15, 22]. The systematic uncertainties are 20% for charge flips, and 50% for both fake and rare SM backgrounds. The $\mathrm{pp} \to \mathrm{t\bar{t}W}$ and $\mathrm{pp} \to \mathrm{t\bar{t}Z}$ production cross-sections used to normalize the Monte Carlo predictions are 232 fb [23] and 208 fb [24, 25], respectively.

5 Event yields

The search is based on comparing the event yields and background predictions in nine signal regions (SRs) with different requirements on $E_{\mathrm{T}}^{\mathrm{miss}}$, H_{T}, and the number of b-tagged jets. In order to improve the sensitivity to $\mathrm{pp} \to \mathrm{tt}$ production, we also define a SR with positive leptons only. The requirements for the SRs are loosely motivated by possible new physics scenarios. For example, signal regions with high $E_{\mathrm{T}}^{\mathrm{miss}}$ are most sensitive to R-parity violating SUSY models with relatively light neutralinos; requiring more H_{T} reduces the SM background while generally maintaining good efficiency to detect new heavy particles that are produced strongly; the signal region with three or more b-tagged jets is sensitive to final states that include several b quarks.

The definition of the signal regions and the results of the search are summarized in Table 2. The basic kinematic properties of the selected events are shown in Fig. 1. The results are consistent with the background predictions. Results with the first 3.95 fb^{-1} of 8 TeV data found 12 out of the 13 events in signal region SR0 and all 11 events in SR1 to have negatively charged leptons (the events in SR1 are a subset of the events in SR0) [26]. The expectation is that around 55% of the selected SM events should have positive leptons (the $\mathrm{t\bar{t}W}$ background results preferentially in positive lepton pairs). The statistical significance of the imbalance of negative versus positive lepton pairs corresponds to 2.6 to 3.7 standard deviations. The actual value depends on whether the probability of the fluctuation is calculated for SR0 or SR1, and for negative leptons only or for both charges. The 7.5 fb^{-1} of data since added yield 13 events with positively charged leptons and 12 with negatively charged leptons in SR1. Thus the total count in SR1 stands at 24 events with leptons with negative charge and 14 events with positively charged leptons. We conclude that the observed charge asymmetry in the first part of the data was most likely due to a statistical fluctuation.

Table 2 also shows the 95% confidence level (CL) observed upper limit (N_{UL}) on the number of non-SM events calculated using the CL_s method [27–29] under three different assumptions for the signal efficiency uncertainty. The limits are only weakly dependent on this uncertainty, which is discussed in Section 6.

We note that some background estimates are obtained using a limited number of sideband events. To compare the predictions in a sample with relatively larger statistics we remove the b-tagging requirement in SR4 ($H_{\mathrm{T}} > 200$ GeV, $MET > 50$ GeV) and relax the requirement on

Table 2: A summary of the combination of results for this search. For each signal region (SR), we show its most distinguishing kinematic requirements, the prediction for the three background (BG) components as well as the total, and the observed number of events. Note that the count of the number of jets on the first line of the table includes both tagged and untagged jets.

No. of jets	≥ 2	≥ 2	≥ 2	≥ 4	≥ 4	≥ 4	≥ 4	≥ 3	≥ 4
No. of btags	≥ 2	≥ 2	≥ 2	≥ 2	≥ 2	≥ 2	≥ 2	≥ 3	≥ 2
Lepton charges	$++/--$	$++/--$	$++$	$++/--$	$++/--$	$++/--$	$++/--$	$++/--$	$++/--$
$E_{\mathrm{T}}^{\mathrm{miss}}$	> 0 GeV	> 30 GeV	> 30 GeV	> 120 GeV	> 50 GeV	> 50 GeV	> 120 GeV	> 50 GeV	> 0 GeV
H_{T}	> 80 GeV	> 80 GeV	> 80 GeV	> 200 GeV	> 200 GeV	> 320 GeV	> 320 GeV	> 200 GeV	> 320 GeV
Charge-flip BG	3.35 ± 0.67	2.70 ± 0.54	1.35 ± 0.27	0.04 ± 0.01	0.21 ± 0.05	0.14 ± 0.03	0.04 ± 0.01	0.03 ± 0.01	0.21 ± 0.05
Fake BG	24.77 ± 12.62	19.18 ± 9.83	9.59 ± 5.02	0.99 ± 0.69	4.51 ± 2.85	2.88 ± 1.69	0.67 ± 0.48	0.71 ± 0.47	4.39 ± 2.64
Rare SM BG	11.75 ± 5.89	10.46 ± 5.25	6.73 ± 3.39	1.18 ± 0.67	3.35 ± 1.84	2.66 ± 1.47	1.02 ± 0.60	0.44 ± 0.39	3.50 ± 1.92
Total BG	39.87 ± 13.94	32.34 ± 11.16	17.67 ± 6.06	2.22 ± 0.96	8.07 ± 3.39	5.67 ± 2.24	1.73 ± 0.77	1.18 ± 0.61	8.11 ± 3.26
Event yield	43	38	14	1	10	7	1	1	9
N_{UL} (13% unc.)	27.2	26.0	9.9	3.6	10.8	8.6	3.6	3.7	9.6
N_{UL} (20% unc.)	28.2	27.2	10.2	3.6	11.2	8.9	3.7	3.8	9.9
N_{UL} (30% unc.)	30.4	29.6	10.7	3.8	12.0	9.6	3.9	4.0	10.5

the number of jets to at least two. The results, summarized in Figure 2, show good agreement between the observed yields and estimated backgrounds.

6 Efficiencies and associated uncertainties

Events are collected with dilepton triggers, with one lepton required to have $p_{\mathrm{T}} > 17$ GeV and the other one $p_{\mathrm{T}} > 8$ GeV. The trigger efficiency, measured using events collected with hadronic triggers, is $96 \pm 5\%$ for ee, $93 \pm 5\%$ for eμ, and $88 \pm 4\%$ for $\mu\mu$. All acceptances calculated from Monte Carlo simulation include a correction factor for the trigger efficiency.

The lepton selection efficiencies, determined using a sample of simulated events from a typical signal scenario involving multiple top final states arising from gluino decay [30, 31], are displayed in Fig. 3. Studies of large samples of $\mathrm{Z} \to$ ee and $\mathrm{Z} \to \mu\mu$ events indicate that the lepton selection efficiencies are reproduced to better than 2% by the simulation. However, leptons in SUSY events have significantly lower isolation efficiency due to the large amount of hadronic activity that is expected in these scenarios. As a result, we conservatively assign an uncertainty of 5% per lepton to the lepton reconstruction efficiency.

The b-tagging efficiency for simulated data is also shown in Fig. 3 for b quarks of $|\eta| < 2.4$ and $p_{\mathrm{T}} > 40$ GeV. The uncertainty on this efficiency is a function of b-jet p_{T}; it is 4.4% at $p_{\mathrm{T}} = 40$ GeV, 2.7% at $p_{\mathrm{T}} = 100$ GeV, and 10% at $p_{\mathrm{T}} = 500$ GeV [17].

The uncertainty on the energy scale of jets in this analysis is also a function of p_{T} [32]. It varies between 5% and 2% in the p_{T} range 40-100 GeV for jets with $|\eta| < 2.4$.

The importance of these effects depends on the signal region and the model of new physics. In general, models with high hadronic activity and large $E_{\mathrm{T}}^{\mathrm{miss}}$ are less affected by the uncertainty on the jet energy scale.

The total uncertainty on the acceptance for the models described in Section 8 is in the 13-20% range. Finally, there is a 4.4% uncertainty on the yield of events from any new physics model due to the uncertainty in the luminosity normalization [33].

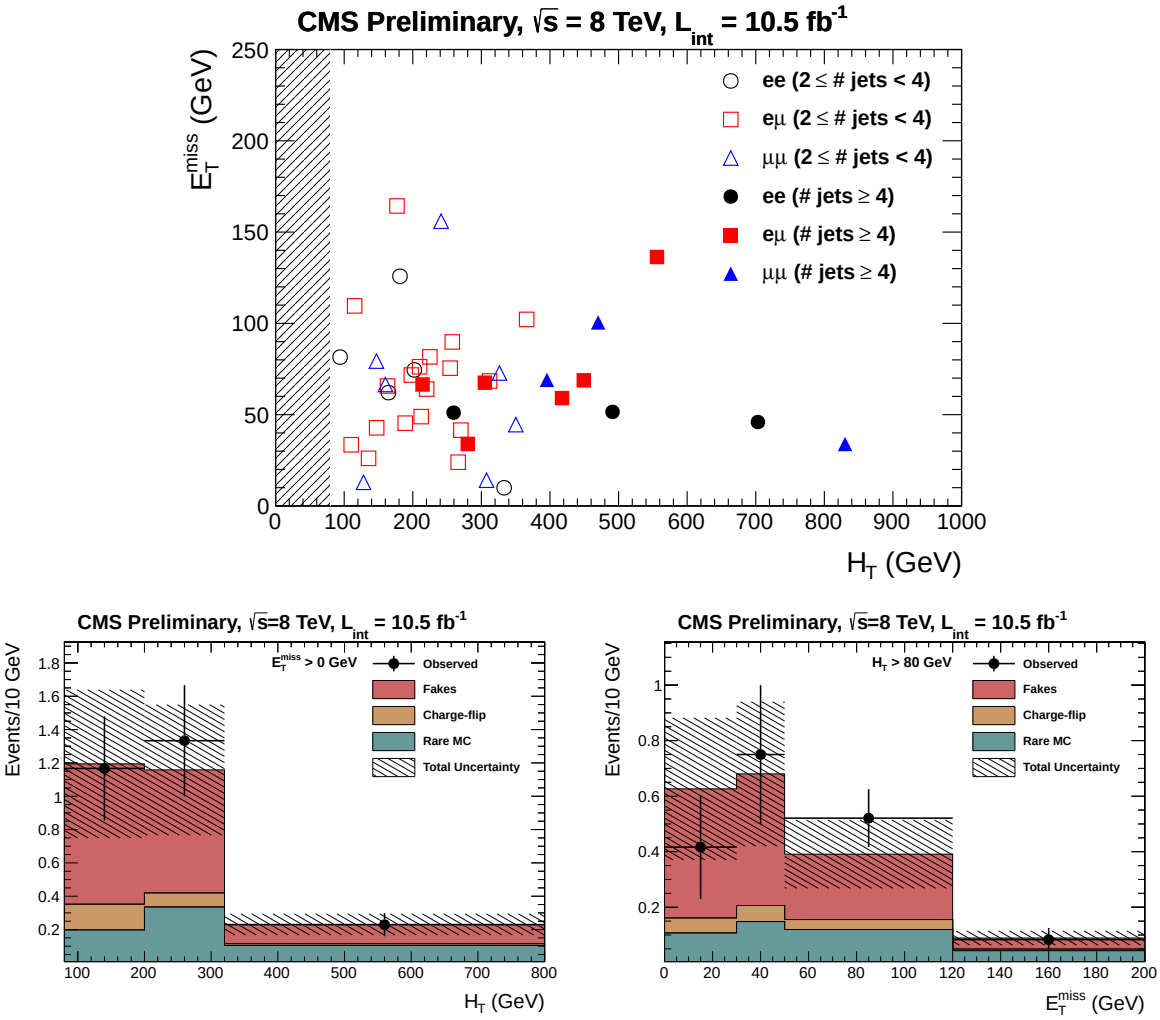

Figure 1: Top plot: distribution of $E_{\mathrm{T}}^{\mathrm{miss}}$ versus H_{T} for the 43 events in the most inclusive signal region (SR0). Note that the ≥ 2 jets requirement in SR0 implies $H_{\mathrm{T}} > 80$ GeV. Bottom-left plot: projection of the scatter plot on the H_{T} axis. Bottom-right plot: projection of the scatter plot on the $E_{\mathrm{T}}^{\mathrm{miss}}$ axis. For the one-dimensional distributions, the number of events in each bin is scaled appropriately to reflect units of events per 10 GeV and is compared with the background predictions, with their uncertainties.

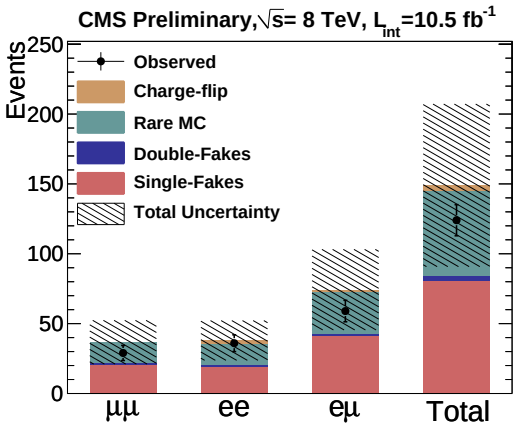

Figure 2: Breakdown of background estimates in a control region. The results are obtained in a region analogous to SR4, but with the b-tagging requirement removed and the requirement on the number of jets relaxed to two in order to obtain a larger statistics sample. The observed yields and estimated backgrounds are in good agreement.

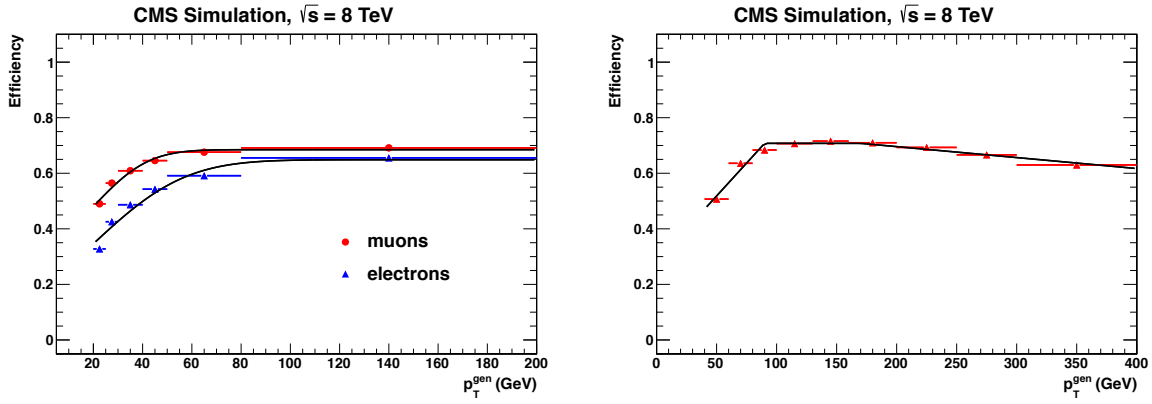

Figure 3: Lepton selection efficiency as a function of p_{T} (left); b-jet tagging efficiency as a function of the b-quark p_{T} (right). The superimposed curves represent the efficiency parametrizations discussed in Section 7.

7 Information for model testing

Our results can be used to confront models of new physics in an approximate way by generator-level studies that compare the expected number of events with the upper limits from Table 2. The "recipe" to be used is given in Ref. [15], Section 7. The $E_{\mathrm{T}}^{\mathrm{miss}}$ and H_{T} turn-on curves in this analysis are the same as those of Ref. [15]. On the other hand the lepton and b-tagging efficiencies are slightly different because of changes in the underlying selections. Their current parametrizations are given below.

The parametrization of the lepton efficiency in Fig. 3 (left) is

$$\epsilon = \epsilon_{\infty}\mathrm{erf}\left(\frac{p_{\mathrm{T}} - 20\,\mathrm{GeV}}{\sigma}\right) + \epsilon_{20}\left[1 - \mathrm{erf}\left(\frac{p_{\mathrm{T}} - 20\,\mathrm{GeV}}{\sigma}\right)\right], \tag{1}$$

with $\epsilon_\infty = 0.65$ (0.69), $\epsilon_{20} = 0.35$ (0.48), and $\sigma = 42$ GeV (25 GeV) for electrons (muons). The parametrization of the simulated b-tagging efficiency, shown in Fig. 3 (right), is $\epsilon = 0.71$ for $90 < p_T < 170$ GeV; at higher (lower) p_T it decreases linearly with a slope of 0.0004 (0.0047) GeV^{-1}.

8 Limits on models of New Physics

The results of the search are used to constrain specific models of new physics. For each model considered, limits are derived from the signal region expected to give the most stringent limit on the cross section at a given point in the parameter space of the model. The event selection efficiency for a given model is obtained from Monte Carlo simulation, and the limits are calculated including systematic uncertainties on lepton efficiency (5% per lepton), trigger efficiency (5%), luminosity (4.4%), jet energy scale, and b-tagging efficiency. The latter two uncertainties are evaluated at each point in the parameter space.

The results from SR1 and SR2 are used to set limits on the cross section for same-sign top quark pair production, $\sigma(pp \to tt + \bar{t}\bar{t})$ from SR1, and $\sigma(pp \to tt)$ from SR2. Here $\sigma(pp \to tt + \bar{t}\bar{t})$ is shorthand for the sum $\sigma(pp \to tt) + \sigma(pp \to \bar{t}\bar{t})$. Note that in most new physics scenarios $pp \to \bar{t}\bar{t}$ is suppressed with respect to $pp \to tt$ because of the parton distribution functions of the proton. These limits are calculated using $pp \to t\bar{t}$ as an acceptance model. The acceptance, including branching fractions, is $0.29 \pm 0.04\%$. We find upper limits $\sigma(pp \to tt + \bar{t}\bar{t}) < 0.87$ pb and $\sigma(pp \to tt) < 0.30$ pb at the 95% CL; the median expected limits are 0.72 and 0.37 pb, respectively.

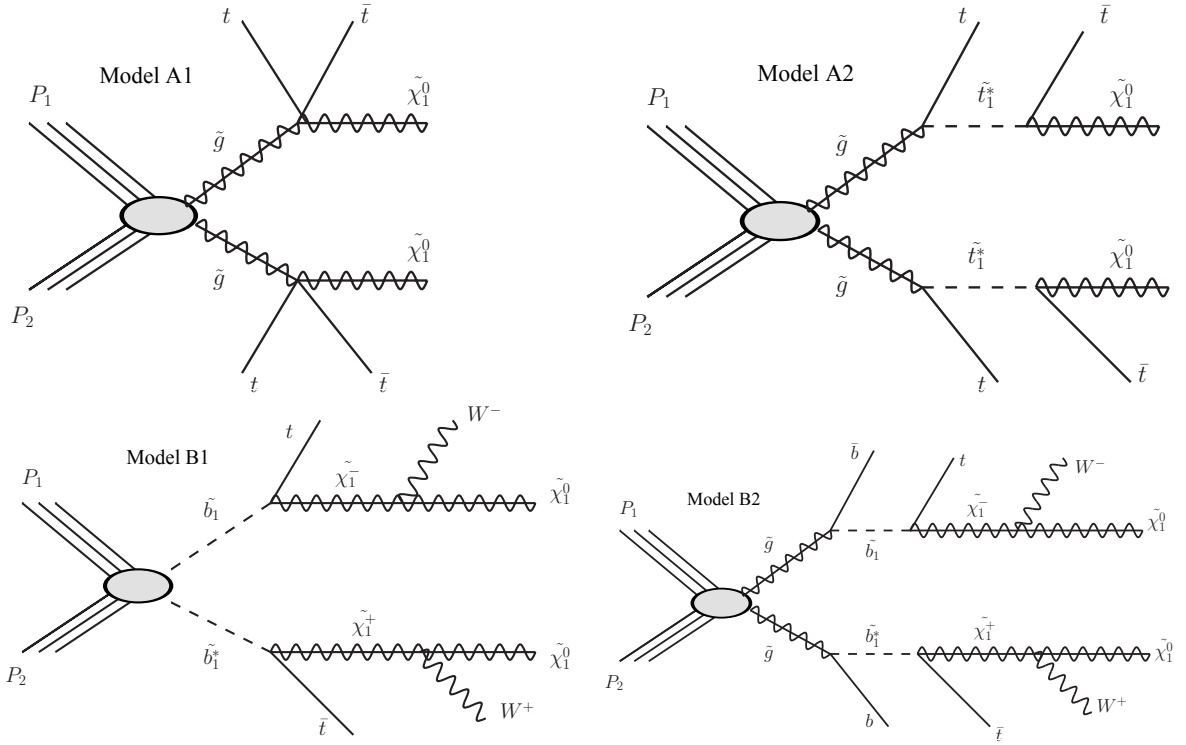

Figure 4: Diagrams for the four SUSY models considered (A1, A2, B1, B2).

Next, we present limits on the parameter spaces of four R-parity conserving SUSY models with third-generation squarks. The decay chains under consideration are shown schematically in Fig. 4.

Scenarios A1 and A2 represent models of gluino pair production resulting in a $\mathrm{tt\bar{t}\bar{t}}\widetilde{\chi}_1^0\widetilde{\chi}_1^0$ final state, where $\widetilde{\chi}_1^0$ is the lightest neutralino [12, 30, 31, 34, 35]. In model A1, the gluino undergoes a three-body decay $\widetilde{\mathrm{g}} \to \mathrm{t\bar{t}}\widetilde{\chi}_1^0$ mediated by an off-shell top squark. In model A2, the gluino decays to antitop-stop, and the on-shell stop further decays into a top quark and a neutralino. The best limit is expected to be given by SR6, except in the scenario of small mass splitting where the best expected limit at times comes from SR3 or SR4.

Models B1 and B2 have bottom squarks decaying as $\widetilde{\mathrm{b}}_1 \to \mathrm{t}\widetilde{\chi}_1^-$ and $\widetilde{\chi}_1^- \to \mathrm{W}^-\widetilde{\chi}_1^0$. Model B1 is a model of sbottom pair production, followed by one of the most likely decay modes of the sbottom; model B2 consists of gluino pair production followed by $\widetilde{\mathrm{g}} \to \widetilde{\mathrm{b}}_1\bar{\mathrm{b}}$. The gluino decay modes in models A1 and A2 would be dominant if the top squark is the lightest supersymmetric quark. Conversely, if the bottom squark is lightest, the decay mode in model B2 would be the most probable. Similar to models A1 and A2, the best expected limit for model B2 is given by SR6. The best limit in the case of Model B1 is not expected to come from any one signal region, instead varying between signal regions 2 through 6 across the sbottom-chargino mass plane.

Excluded regions in the parameter space of the four models are shown in Fig. 5. For the gluino-initiated models (A1, A2, and B2), we exclude gluinos with masses below around 970 GeV, with a small dependence on the details of the models. This is because the limits are driven by the common gluino pair production cross-section. In the case of sbottom pair production (model B1) we set a limit $m(\widetilde{\mathrm{b}}_1) > 445$ GeV at 95% CL.

These models are also probed by other CMS new physics searches in different decay modes, although other searches have so far been interpreted in the context of model A1 but not A2, B1, or B2. For model A1 the limits given here are complementary to the limits from the single-lepton and "razor" searches [36]: less stringent at low $m(\widetilde{\chi}_1^0)$ but more stringent at high $m(\widetilde{\chi}_1^0)$. A similar conclusion would apply to model A2, since the final state is the same. Comparable limits for model A1, as well as for similar models with top and bottom quarks from gluino decays, have been reported by the ATLAS collaboration [37–39]. In the case of sbottom pair production, the ATLAS collaboration has reported a limit $m(\widetilde{\mathrm{b}}_1) > 390$ GeV, but assuming the decay mode $\widetilde{\mathrm{b}}_1 \to \mathrm{b}\widetilde{\chi}_1^0$ instead of the model B1 mode $\widetilde{\mathrm{b}}_1 \to \mathrm{t}\widetilde{\chi}_1^-$ [40].

9 Summary

We have presented results of a search for same-sign dileptons with b-jets using the CMS detector at the LHC based on a 10.5 fb^{-1} data sample of pp collisions at $\sqrt{s}$ = 8 TeV. No significant deviations from the SM expectations are observed.

The results are used to set upper limit on the same-sign top cross-section $\sigma(\mathrm{pp} \to \mathrm{tt} + \mathrm{\bar{t}\bar{t}}) < 0.87$ pb and $\sigma(\mathrm{pp} \to \mathrm{tt}) < 0.30$ pb at the 95% CL.

We also exclude gluinos with masses up to approximately 970 GeV if they decay exclusively into stop pairs or sbottom pairs. Finally, we place a lower limit on the bottom squark mass of 445 GeV. Note that, as is often the case, the limits on SUSY particles are model dependent, since we have assumed that the stop and sbottom decay as $\widetilde{\mathrm{t}}_1 \to \mathrm{t}\widetilde{\chi}_1^0$ and $\widetilde{\mathrm{b}}_1 \to \mathrm{t}\widetilde{\chi}_1^-$, respectively. In the latter case we have also assumed $\widetilde{\chi}_1^- \to \mathrm{W}^-\widetilde{\chi}_1^0$.

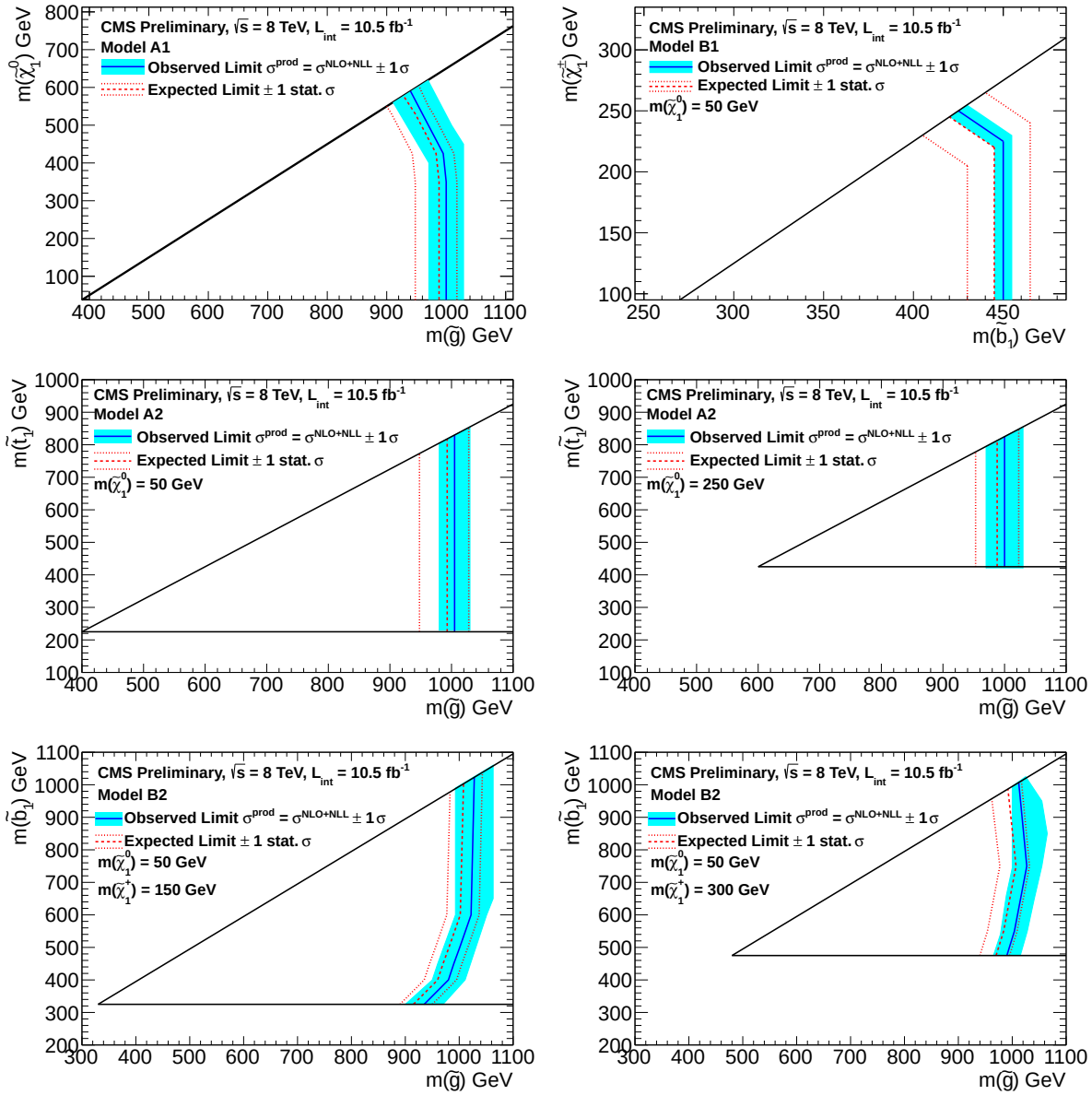

Figure 5: Exclusion regions at 95% CL in the planes of $m(\widetilde{\chi}_1^0)$ vs. $m(\widetilde{\mathrm{g}})$ (model A1), $m(\widetilde{\chi}_1^-)$ vs. $m(\widetilde{\mathrm{b}}_1)$ (model B1), $m(\widetilde{\mathrm{t}}_1)$ vs. $m(\widetilde{\mathrm{g}})$ (model A2), and $m(\widetilde{\mathrm{b}}_1)$ vs. $m(\widetilde{\mathrm{g}})$ (model B2). Models A2, B1, and B2 have more than two mass parameters, and cannot be fully represented in a two dimensional plot. The assumed values of the additional mass parameters are indicated in the plots. The black lines represent the kinematic boundaries of the models. The excluded regions are those within the kinematic boundaries and to the left of the lines. The effects of the theoretical uncertainties on the next-to-leading-order plus next-to-leading-log calculations of the production cross-sections [41] are indicated by the shaded bands.

References

[1] R. M. Barnett, J. F. Gunion, and H. E. Haber, "Discovering supersymmetry with like sign dileptons", *Phys. Lett.* **B315** (1993) 349–354, doi:10.1016/0370-2693(93)91623-U, arXiv:hep-ph/9306204.

[2] M. Guchait and D. Roy, "Like sign dilepton signature for gluino production at CERN LHC including top quark and Higgs boson effects", *Phys. Rev.* **D52** (1995) 133–141, doi:10.1103/PhysRevD.52.133, arXiv:hep-ph/9412329.

[3] H. Baer, C.-h. Chen, F. Paige et al., "Signals for minimal supergravity at the CERN large hadron collider. 2: Multi - lepton channels", *Phys. Rev.* **D53** (1996) 6241–6264, doi:10.1103/PhysRevD.53.6241, arXiv:hep-ph/9512383.

[4] H.-C. Cheng, K. T. Matchev, and M. Schmaltz, "Bosonic supersymmetry? Getting fooled at the CERN LHC", *Phys. Rev.* **D66** (2002) 056006, doi:10.1103/PhysRevD.66.056006, arXiv:hep-ph/0205314.

[5] R. Contino and G. Servant, "Discovering the top partners at the LHC using same-sign dilepton final states", *JHEP* **0806** (2008) 026, doi:10.1088/1126-6708/2008/06/026, arXiv:0801.1679.

[6] J. Almeida, F.M.L., Y. D. A. Coutinho, J. A. Martins Simões et al., "Same sign dileptons as a signature for heavy Majorana neutrinos in hadron hadron collisions", *Phys. Lett.* **B400** (1997) 331–334, doi:10.1016/S0370-2693(97)00143-3, arXiv:hep-ph/9703441.

[7] Y. Bai and Z. Han, "Top-antitop and Top-top Resonances in the Dilepton Channel at the CERN LHC", *JHEP* **0904** (2009) 056, doi:10.1088/1126-6708/2009/04/056, arXiv:0809.4487.

[8] E. L. Berger, Q.-H. Cao, C.-R. Chen et al., "Top Quark Forward-Backward Asymmetry and Same-Sign Top Quark Pairs", *Phys. Rev. Lett.* **106** (2011) 201801, doi:10.1103/PhysRevLett.106.201801, arXiv:1101.5625.

[9] A. G. Cohen, D. Kaplan, and A. Nelson, "The More minimal supersymmetric standard model", *Phys. Lett.* **B388** (1996) 588, doi:10.1016/S0370-2693(96)01183-5, arXiv:hep-ph/9607394.

[10] S. Dimopoulos and G. Giudice, "Naturalness constraints in supersymmetric theories with nonuniversal soft terms", *Phys. Lett.* **B357** (1995) 573, doi:10.1016/0370-2693(95)00961-J, arXiv:hep-ph/9507282.

[11] R. Barbieri, G. Dvali, and L. J. Hall, "Predictions from a U(2) flavor symmetry in supersymmetric theories", *Phys. Lett.* **B377** (1996) 76, doi:10.1016/0370-2693(96)00318-8, arXiv:hep-ph/9512388.

[12] M. Papucci, J. T. Ruderman, and A. Weiler, "Natural SUSY Endures", (2011). arXiv:1110.6926.

[13] C. Csaki, L. Randall, and J. Terning, "Light Stops from Seiberg Duality", (2012). arXiv:1201.1293.

[14] CMS Collaboration, "The CMS experiment at the CERN LHC", *JINST* **3** (2008) S08004, doi:10.1088/1748-0221/3/08/S08004.

[15] CMS Collaboration, "Search for new physics in events with same-sign dileptons and b-tagged jets in pp collisions at sqrt(s) = 7 TeV", *JHEP* **1208** (2012) 110, doi:10.1007/JHEP08(2012)110, arXiv:1205.3933.

[16] CMS Collaboration, "Particle–Flow Event Reconstruction in CMS and Performance for Jets, Taus, and $E_{\mathrm{T}}^{\mathrm{miss}}$", CMS Physics Analysis Summary CMS-PAS-PFT-09-001, (2009).

[17] CMS Collaboration, "Identification of b-quark jets in the CMS experiment",. in preparation.

[18] J. Alwall, P. Demin, S. de Visscher et al., "MadGraph/MadEvent v4: The New Web Generation", *JHEP* **0709** (2007) 028, doi:10.1088/1126-6708/2007/09/028, arXiv:0706.2334.

[19] T. Sjostrand, S. Mrenna, and P. Z. Skands, "PYTHIA 6.4 Physics and Manual", *JHEP* **0605** (2006) 026, doi:10.1088/1126-6708/2006/05/026, arXiv:hep-ph/0603175.

[20] GEANT4 Collaboration, "GEANT4–a simulation toolkit", *Nucl. Instrum. Meth. A* **506** (2003) 250, doi:10.1016/S0168-9002(03)01368-8.

[21] S. Abdullin, P. Azzi, F. Beaudette et al., "The fast simulation of the CMS detector at LHC", *J.Phys.Conf.Ser.* **331** (2011) 032049, doi:10.1088/1742-6596/331/3/032049.

[22] CMS Collaboration, "Search for new physics with same-sign isolated dilepton events with jets and missing transverse energy at the LHC", *JHEP* **1106** (2011) 077, doi:10.1007/JHEP06(2011)077, arXiv:1104.3168.

[23] J. M. Campbell and R. K. Ellis, "$t\bar{t}W^{\pm}$ production and decay at NLO", (2012). arXiv:1204.5678.

[24] A. Kardos, Z. Trocsanyi, and C. Papadopoulos, "Top quark pair production in association with a Z-boson at NLO accuracy", *Phys. Rev.* **D85** (2012) 054015, doi:10.1103/PhysRevD.85.054015, arXiv:1111.0610.

[25] M. Garzelli, A. Kardos, C. Papadopoulos et al., "Z0 - boson production in association with a top anti-top pair at NLO accuracy with parton shower effects", *Phys.Rev.* **D85** (2012) 074022, doi:10.1103/PhysRevD.85.074022, arXiv:1111.1444.

[26] CMS Collaboration, "Search for new physics in events with same-sign dileptons and b-tagged jets in pp collisions at $sqrts = 8$ TeV", CMS Physics Analysis Summary CMS-PAS-SUS-12-017, (2012).

[27] T. Junk, "Confidence level computation for combining searches with small statistics", *Nucl. Instrum. Meth.* **A434** (1999) 435, doi:10.1016/S0168-9002(99)00498-2, arXiv:hep-ex/9902006.

[28] ATLAS and CMS Collaborations, "Procedure for the LHC Higgs boson search combination in summer 2011", ATL-PHYS-PUB-2011-011, CMS NOTE-2011/005, (2011).

[29] A. L. Read, "Presentation of search results: The CL(s) technique", *J.Phys.* **G28** (2002) 2693–2704, doi:10.1088/0954-3899/28/10/313.

[30] LHC New Physics Working Group Collaboration, "Simplified Models for LHC New Physics Searches", (2011). arXiv:1105.2838. Model of Section IV.E with topology (B+B).

[31] R. Essig, E. Izaguirre, J. Kaplan et al., "Heavy Flavor Simplified Models at the LHC", *JHEP* **1201** (2012) 074, doi:10.1007/JHEP01(2012)074, arXiv:1110.6443.

[32] CMS Collaboration, "Determination of Jet Energy Calibration and Transverse Momentum Resolution in CMS", *JINST* **6** (2011) P11002, doi:10.1088/1748-0221/6/11/P11002, arXiv:1107.4277.

[33] CMS Collaboration, "CMS luminosity based on pixel cluster counting - Summer 2012 Update", technical report, (2012).

[34] B. S. Acharya, P. Grajek, G. L. Kane et al., "Identifying Multi-Top Events from Gluino Decay at the LHC", (2009). arXiv:0901.3367.

[35] G. L. Kane, E. Kuflik, R. Lu et al., "Top Channel for Early SUSY Discovery at the LHC", *Phys. Rev.* **D84** (2011) 095004, doi:10.1103/PhysRevD.84.095004, arXiv:1101.1963.

[36] CMS Collaboration, "Interpretation of Searches for Supersymmetry with Simplified Models", (2012). in preparation.

[37] ATLAS Collaboration, "Search for gluinos in events with two same-sign leptons, jets and missing transverse momentum with the ATLAS detector in pp collisions at sqrt(s) = 7 TeV", *Phys. Rev. Lett.* **108** (2012) 241802, arXiv:1203.5763.

[38] ATLAS Collaboration, "Search for supersymmetry in pp collisions at sqrt(s) = 7 TeV in final states with missing transverse momentum and b-jets with the ATLAS detector", *Phys. Rev.* **D85** (2012) 112006, arXiv:1203.6193.

[39] ATLAS Collaboration, "Search for top and bottom squarks from gluino pair production in final states with missing transverse energy and at least three b-jets with the ATLAS detector", arXiv:1207.4686.

[40] ATLAS Collaboration, "Search for scalar bottom pair production with the ATLAS detector in pp Collisions at sqrts = 7 TeV", *Phys. Rev. Lett.* **108** (2012) 181802, doi:10.1103/PhysRevLett.108.181802, arXiv:1112.3832.

[41] M. Krämer, A. Kulesza, R. van der Leeuw et al., "Supersymmetry production cross sections in pp collisions at sqrts = 7 TeV", (2012). arXiv:1206.2892.